HOT DEFORMATION BEHAVIOUR AND MICROSTRUCTURAL EVOLUTION OF BIMODAL SIZE PARTICULATES REINFORCED ($TiB+La_2O_3$)/Ti COMPOSITES

Xianglong Sun, Yuanfei Han*, Liqiang Wang, Weijie Lu*

State Key Laboratory of Metal Matrix Composites, Shanghai Jiao Tong University, Shanghai 200240, China

*Corresponding author: Tel.: +86-21-34202641; Fax: +86-21-34202749

Email address: hyuf1@hotmail.com (Yuanfei Han); luweijie@sjtu.edu.cn (Weijie Lu)

Keywords: Titanium matrix composites, Hot deformation behaviour, Processing map, Dynamic recrystallization

In the past decades, the proportion of high temperature titanium alloy in aeroengine components gradually increases with the development of high thrust-weight ratio aeroengine. However, the elevated temperature strength and creep strength of titanium alloy decrease above 600 ℃, which limits the development of the titanium alloy in a higher service temperature [1-6]. Comparing with conventional titanium alloys, titanium matrix composites (TMCs) have many excellent properties such as low density, high specific strength, good resistance to elevated temperatures and corrosion resistance, which possess the great potential application for higher temperature fields [7-9]. However, the deformation resistance increases inevitably with introducing reinforcements into titanium alloy. Therefore, it is necessary to further study the hot deformation behaviour of TMCs due to the narrow processing window.

Many researches about the hot deformation behaviour and microstructural evolution of various TMCs have been carried out. Wang et al. [10] investigated the hot deformation behavior of TiB/Ti60 composites with a network microstructure, and the constitutive equation and processing maps were established in terms of the flow stress curves. The deformation mechanism in the safe domain corresponded to dynamic recrystallization of lamella α phase while inhomogeneous deformation and macroscopic crack were observed in the instable domain. In Poletti's study [11], the processing maps of TiB/Ti-6Al-4V composites using the modified DMM correlated well with the different deformation mechanisms, which were conducive to the optimization of hot working parameters. And superplasticity in the safe domain and cracking or debonding of larger TiB in the instable domain were observed. However, the previous studies were mainly concerned about the composites reinforced by the micron-scale reinforcements such as TiB whiskers and TiC particles. TMCs reinforced by the single size reinforcement had shown enormous superiority in high specific strength while the ductility was damaged. But the excellent comprehensive properties including high specific strength, good ductility, good resistance to elevated temperatures and creep resistance have been found in TMCs reinforced by micron-scale TiB whiskers and nano-scale La_2O_3 particles. Nevertheless, the study about hot deformation behaviour of bimodal size particulates

reinforced (TiB+La_2O_3)/Ti composites has not been reported.

In this work, near-α titanium alloy (IMI834) was selected as matrix, and TiB whiskers and La_2O_3 particles were selected as reinforcements. In order to investigate the hot deformation behaviour and microstructural evolution of the bimodal size particulates reinforced (TiB+La_2O_3)/Ti composites, the isothermal compression were carried out at the temperatures range of 850-1100℃ and strain rates range of 0.001-1s^{-1} with true strain of 0.92. The microstructures with different deformation condition were observed by optical microscope (OM), scanning electron microscope (SEM), transmission electron microscope (TEM) and electron back-scattered diffraction (EBSD).

The flow stress curves of (TiB+La_2O_3)/Ti composites under different deformation parameters were shown in Fig.1. It can be seen that the composites exhibited the remarkable temperature sensitivity and strain rate sensitivity, and the flow stress increased with decreasing temperature or increasing strain rate in the α+β phase region (850℃-950℃) or β phase region (1050℃-1100℃). In the β phase region, the dynamic equilibrium between dislocation multiplication and disappearance was achieved, which showed the significant steady-state characteristics. However, the steady-state in the α+β phase region is not obvious, mainly due to the dynamic recrystallization, superplasticity or reinforcement breaking, which leads to the decrease of the flow stress.

The constitutive equation during α+β phase region and β phase region was established based on flow stress data at different temperatures and strain rates. The apparent activation energy was calculated to be 752 kJ/mol in α+β phase region and 185 kJ/mol in β phase region, which were much higher than those of matrix alloy (α+β phase region: 703 kJ/mol, β phase region: 153 kJ/mol) due to the hard deformation caused by the bimodal size reinforcements. According to the dynamic material model, the processing maps of (TiB+La_2O_3)/Ti composites were established, as shown in Fig. 2. It can be seen that there are two power dissipation peak regions ($\eta > 40\%$) in the processing map, which are located in the α+β phase region (900-950℃, 0.003-0.1s^{-1}) and β single phase region (1075-1100℃, 0.3-1s^{-1}), corresponding to the safe domain in hot working. In addition, the instability domain was located at 850-975℃/0.1-1s^{-1}, corresponding to the low power dissipation area.

The macro appearance of (TiB+La_2O_3)/Ti composites after isothermal compression was shown in Fig.3. The deformed specimens under different deformation conditions showed the round-cake shape without obvious fracture, which indicated that the composites have good plasticity. By observing the cross section of the specimen, it can be found that the reinforcements were distributed in the flow line after the compression deformation, and the center of the specimen suffered the most severe deformation. As shown in Fig. 4a, the microstructure of as-forged (TiB+La_2O_3)/Ti composites mainly consists of the primary α phase distributed on the β-transformation matrix and the TiB reinforcement arranged in the forging direction. Fig. 4b showed the microstructure of (TiB+La_2O_3)/Ti composites after compression deformation at 900℃/1s^{-1}. It can be seen that inhomogeneous deformation and breaking or interfacial debonding of TiB whiskers were obvious, indicating that the composites were not suitable for deforming at low temperature and high strain rate. With the increase of deformation temperature, a large number of lamellar α phases appeared and further produced obvious spheroidization at higher strain rate (Fig. 4c). The results of EBSD showed that the primary α phase and lamellar α phase produced the dynamic recrystallization

(DRX) at 950℃/0.1s^{-1}, resulting in a large amount of fine recrystallized grains (Fig. 4d). Additionally, Fig. 4e exhibited that there are 67.6% high-angle grain boundaries (HAGBs, >15°) and 32.4% low-angle grain boundaries (LAGBs, <15°) in the deformed microstructure at 950℃/0.1s^{-1}, which indicates that new DRXed grains are developed by the in situ evolution of subgrains with the growth of LAGBs to HAGBs, which is associated with the typical continuous dynamic recrystallization (CDRX) mechanism.

When the deformation was completely carried out in the β single phase region, all the primary α phase transformed into β phase, as shown in Fig. 5a. The coarse β grains were compressed and showed the flat shape along the flow direction of the metal. With increasing the degree of deformation, the dynamic recrystallization was occurred in β phase, and the recrystallized β grains gradually precipitated at the grain boundary and formed the incomplete recrystallization characteristics. But the non-uniformity in microstructure was harmful to obtain the forgings with the excellent performance. During the subsequent cooling process, the lamellar α occurred along the β grain boundary. Simultaneously, a large number of tangled dislocations shown in Fig. 5b can promote the formation of the cell structure, which indicated that the main deformation mechanism of lamellar α phase was the dynamic recovery.

Based on the above analysis, the appropriate hot working window corresponded to the stability domain (900-950℃/0.003-0.1s^{-1}). The continuous dynamic recrystallization of primary α grains and dynamic globularization of lamellar α (α+β phase region), necklace recrystallization of β grains and dynamic recovery of lamellar α (β phase region) were the deformation mechanisms.

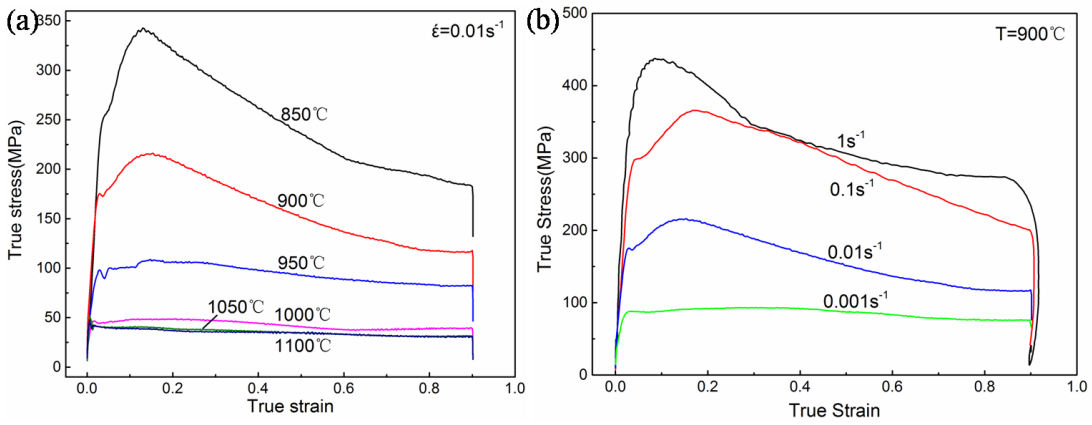

Figure 1: Flow stress curves of (TiB+La_2O_3)/Ti composites at (a) the strain rate is 0.01s^{-1}, (b) the deformation temperature is 900℃

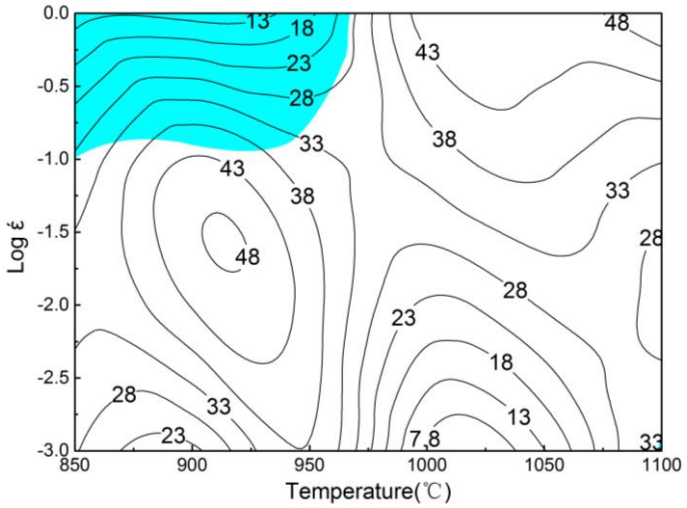

Figure 2: The processing map of (TiB+La_2O_3)/Ti composites at true strain of 0.7 (the blue domain represents the instability domain)

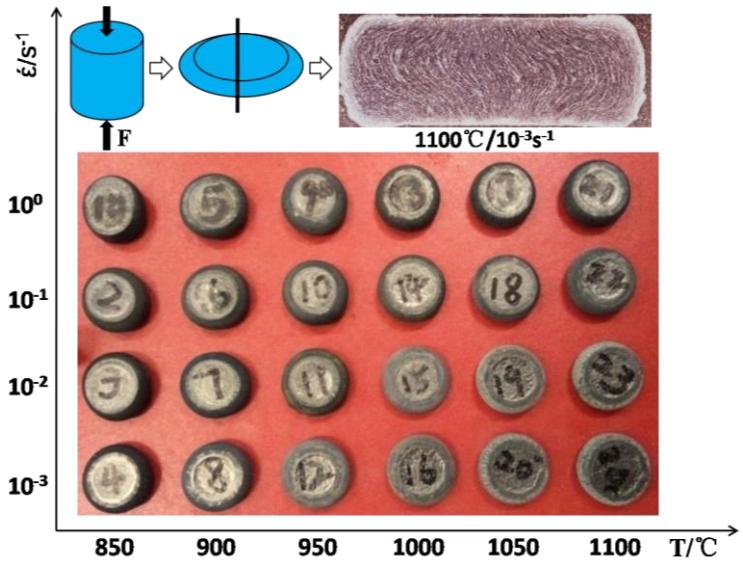

Figure 3: The macro appearance of (TiB+La_2O_3)/Ti composites after the isothermal compressing tests

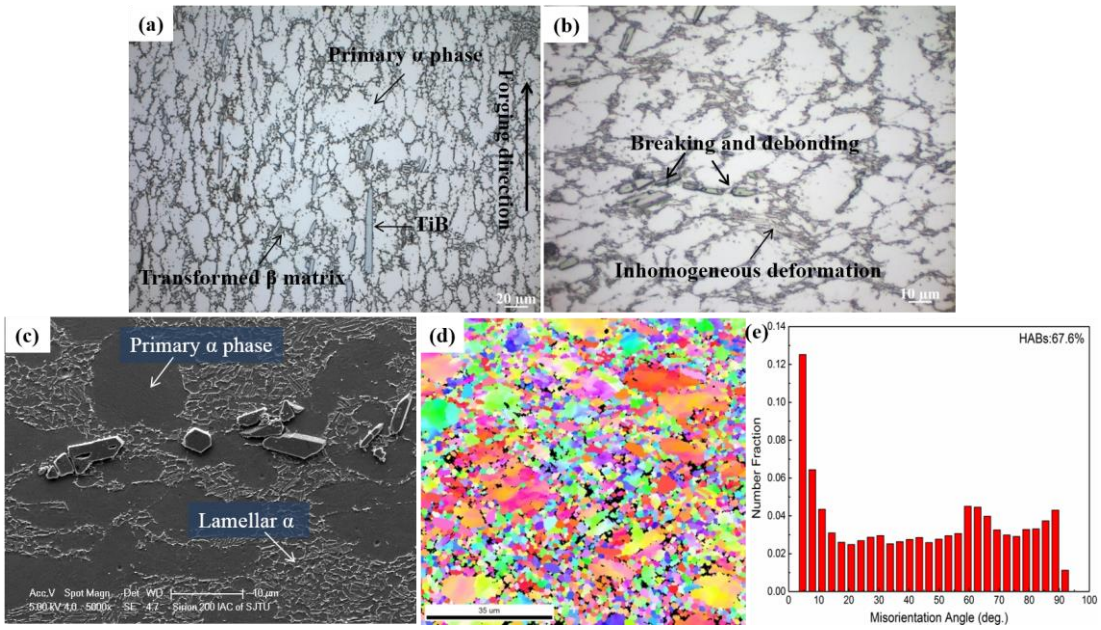

Figure 4: (a) Optical micrograph of initial microstructure, (b) SEM micrograph at 900℃/1s^{-1}, (c) SEM micrograph at 950℃/0.1s^{-1}, (d) IPF map at 950℃/0.1s^{-1} and (e) Misorientation angle distribution at 950℃/0.1s^{-1}

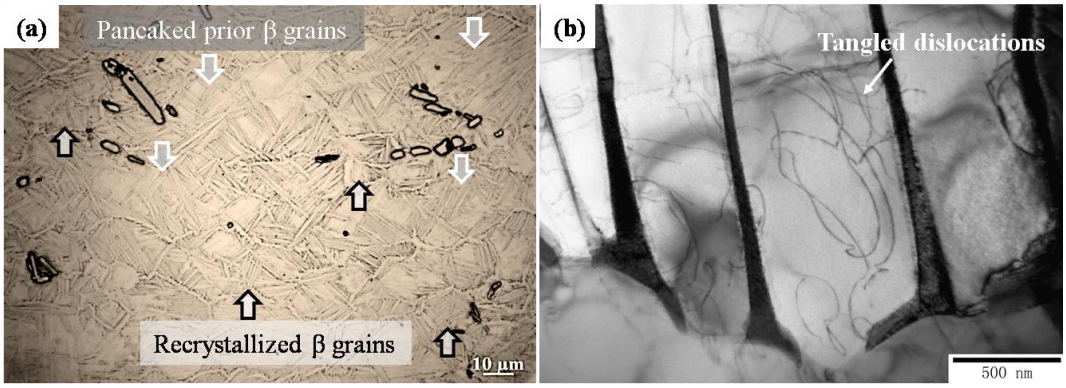

Figure 5: Micrographs of (TiB+La_2O_3)/Ti composites deformed at 1100℃/1s^{-1} (a) OM and (b) TEM

REFERENCES

[1] Es-Souni M. Creep behaviour and creep microstructures of a high-temperature titanium alloy Ti–5.8 Al–4.0 Sn–3.5 Zr–0.7 Nb–0.35 Si–0.06 C (Timetal 834): part I. Primary and steady-state creep[J]. Materials characterization, 2001, 46(5): 365-379.

[2] Hardt S, Maier H J, Christ H J. High-temperature fatigue damage mechanisms in near-α titanium alloy IMI 834[J]. International journal of fatigue, 1999, 21(8): 779-789.

[3] Kumar A, Singh N, Singh V. Influence of stabilization treatment on low cycle fatigue behavior of Ti alloy IMI 834[J]. Materials characterization, 2003, 51(4): 225-233.

[4] Germain L, Gey N, Humbert M, et al. Analysis of sharp microtexture heterogeneities in a bimodal IMI 834 billet[J]. Acta Materialia, 2005, 53(13): 3535-3543.

[5] Xiao L, Lu W, Yang Z, et al. Effect of reinforcements on high temperature mechanical properties of in situ synthesized titanium matrix composites[J]. Materials Science and

Engineering: A, 2008, 491(1): 192-198.
[6] Wang B, Huang L J, Geng L, et al. Compressive behaviors and mechanisms of TiB whiskers reinforced high temperature Ti60 alloy matrix composites[J]. Materials Science and Engineering: A, 2015, 648: 443-451.
[7] W.J. Lu, D. Zhang, X. Zhang, R.J. Wu, T. Sakata, H. Mori, HREM study of TiB/Ti interfaces in a TiB-TiC in situ composite, Scr. Mater. 44 (2001) 1069-1075.
[8] H.Q. Duan, Y.F. Han, W.J. Lu, L.Q. Wang, J.W. Mao, D. Zhang, Configuration design and fabrication of laminated titanium matrix composites, Mater. Des. 99 (2016) 219-224.
[9] H.T. Tsang, C.G. Chao, C.Y. Ma, In situ fracture observation of a TiC/Ti MMC produced by combustion synthesis, Scr. Mater. 35 (1996) 1007-1012.
[10] Wang B, Huang L J, Geng L, et al. Compressive behaviors and mechanisms of TiB whiskers reinforced high temperature Ti60 alloy matrix composites[J]. Materials Science and Engineering: A, 2015, 648: 443-451.
[11] Poletti C, Warchomicka F, Degischer H P. Local deformation of Ti6Al4V modified 1wt% B and 0.1 wt% C[J]. Materials Science and Engineering: A, 2010, 527(4): 1109-1116.